Journal of Organometallic Chemistry, *455* (1993) 167–175

JOM 23562

Synthesis and structure of acylcarbonylindenyl(phosphine)iron(II) complexes. Analysis of ligand effects in an indenyl system

Lucia Ambrosi, Mauro Bassetti, Patrizia Buttiglieri, Luisa Mannina and Donato Monti
Centro C.N.R. di Studio sui Meccanismi di Reazione, c/o Dipartimento di Chimica, Universita' "La Sapienza", 00185 Roma (Italy)

Gabriele Bocelli
Centro C.N.R. di Studio per la Strutturistica Diffrattometrica, Viale delle Scienze, 43100 Parma (Italy)

(Received January 13, 1993)

Abstract

The reactions of $(C_9H_7)Fe(CO)_2R$ ($R = CHMe_2$, Me) with phosphines and phosphites (L) yield two series of indenyl complexes $(C_9H_7)Fe(CO)(COR)(L)$ *via* the migratory insertion process. The acyl complexes provide a case of diastereotopic shielding by an asymmetric iron atom. The phosphorus ligands exert electronic effects on the terminal carbonyl group of the methyl complexes that are essentially the same in the indenyl system and in the analogous cyclopentadienyl system. Substitution of methyl for isopropyl in the acyl moiety increases π-back bonding from iron to carbonyl. The structure of $(C_9H_7)Fe(CO)(COCHMe_2)(PPh_3)$ has been determined by X-ray analysis, and exhibits a distorted η^5 coordination of the indenyl ligand [slip value = 0.122 Å (mean *d*(Fe–C(3a), C(7a)) – mean *d*(Fe–C(1), C(3))].

1. Introduction

Increasing interest has been devoted to the ability of (η^5-indenyl) transition-metal complexes to promote reactions that involve association with nucleophiles. Substitution of the η^5-indenyl group by η^5-cyclopentadienyl produces rate enhancements in both carbonyl-substitution reactions [1] and migratory-insertion reactions [2]. The higher reactivity of the indenyl system has been generally interpreted in terms of readily accessible η^3-intermediates [3]. According to this interpretation, the formation of these species allows delocalization of electron density from the entering group into the fused benzene ring which regains full aromaticity and stabilizes the intermediate, providing a reaction pathway lower in energy than that of the corresponding cyclopentadienyl systems. In contrast, it has been reported that complexes containing indenyl are 10–15 kcal mol^{-1} less stable than those of cyclopentadienyl, and that the higher reactivity may largely depend on this greater ground-state destabilization [4].

Cyclopentadienyliron(II) complexes have been studied in great detail, especially the influence of phosphorus ligands, which affect bonding, structure, thermodynamics and kinetics [5]. Similar systematic studies on indenyliron(II) complexes should result in more information concerning the ground-state and excited-state properties of both systems, and allow meaningful comparisons in terms of structure and reactivity. The structures and spectroscopic properties of $[(C_9H_7)_2M]$ (M = Fe, Co or Ni) have recently been reported and compared with those of the corresponding cyclopentadienyl complexes [6]. We now report on the synthesis and properties of a series of acyl complexes $[(C_9H_7)Fe(CO)(COR)(L)]$, products of the migratory insertion reaction induced by phosphorus donors (L) in the alkyl complexes $[(C_9H_7)Fe(CO)_2R]$ ($R = CHMe_2$ or Me). Phosphorus ligands are important in the study of migratory insertions [7]. In addition, the existence of several parameters that accurately define steric and electronic features make the Group 15 donors the most suitable class for structural and mechanistic studies of transition metal complexes [8].

Correspondence to: Dr. M. Bassetti or Dr. G. Bocelli.

0022-328X/93/$6.00

2. Results and discussion

2.1. Synthesis and properties

The indenyl complexes $[(C_9H_7)Fe(CO)_2R]$ served as our starting materials for the preparation of a series of acylcarbonylindenyl-iron(II) complexes $[(C_9H_7)Fe(CO)(L)(COR)]$ (**1–19a**, R = $CHMe_2$; **2–19b**, R = Me; L = phosphines or phosphites). The alkyl complexes react with phosphorus donors in toluene *via* a migratory insertion reaction of carbon monoxide (eqn. (1)).

$$[(C_9H_7)Fe(CO)_2R] + L \xrightarrow{\text{toluene}} [(C_9H_7)Fe(CO)(COR)(L)] \qquad (1)$$

$$R = CHMe_2,\ \text{room temperature, 12 h}$$

$$R = Me,\ 50\text{–}60°C,\ 24\ h$$

The infrared data of the new acyl complexes **1–19a,b** are reported in Table 1, along with the steric and electronic parameters of the phosphorus ligands (L). Consistent with the greater migratory aptitude of the isopropyl group compared with methyl, showed by kinetic studies on $[CpFe(CO)_2R]$ (Cp = C_5H_5) [9], the reactions of $[(C_9H_7)Fe(CO)_2(CHMe_2)]$ proceed smoothly at room temperature, and form the corresponding acyl complexes in higher yields than those obtained from the methyl complex. The products were separated from the crude reaction mixture by column chromatography, and obtained in yields ranging from 50% to 80%.

In the indenyl complexes $[(C_9H_7)Fe(CO)(COCHMe_2)(L)]$, the phosphorus ligand cone angles, θ, varies from 101° [**1**, $P(OCH_2)_3CEt$] to 170° (**19**, PCy_3, Cy = cyclohexyl) and the pK_a values, from −2.0 [**6**, $P(OPh)_3$] to 9.70 (**19**, PCy_3). The reaction with $P(^tBu)_3$ does not proceed at room temperature and produces a complex mixture of products at 80°C, among which the acyl complex cannot be detected. Since $P(^tBu)_3$ is the most basic ($pK_a = 11.4$), the lack of reactivity is a result of the large cone angle (182°). Therefore, the steric threshold for the reaction of the isopropyl complex is between 170° (PCy_3) and 182°. The same result was found for the reactions of the cyclopentadienylmethyl complex $[(Cp)Fe(CO)_2Me]$ [5a]. Evidently, the greater size of both the indenyl moiety and the isopropyl group does not reduce the ability of the iron complexes to bind large ligands.

The acylindenyl complexes prepared in this study have a single sharp ν(CO) IR band, in contrast to the complexes $[(Cp)Fe(CO)(COMe)(L)]$ which have θ values larger than 152°. These exist in solution as rapidly interconverting isomers, and exhibit two or three ν(CO) bands [5a]. Because $[(C_9H_7)Fe(CO)(COMe)(PBzPh_2)]$ (**17b**) also shows two carbonyl bands, the existence of a single species, even in the case of large ligands, is related to the presence of the isopropyl group, which probably freezes the complex in a single structure.

Because the complexes **1–19a,b** are chiral, the two halves of the indenyl ligand and the two methyl groups of the isopropyl moiety are diastereotopic. This is manifested in both the ^1H and ^{13}C NMR spectra. The

TABLE 1. Terminal carbonyl, ν(CO), and acyl-stretching frequencies, ν(COR), of $[(C_9H_7)Fe(CO)(COR)(L)]$ in cyclohexane (±0.2 cm^{-1}), and steric and electronic parameters of phosphorus ligand (L)

	L	R = $CHMe_2$		R = Me				
		ν(CO)	ν(COR)	ν(CO)	ν(COR)	θ [a]	pK_a [b]	χ [b]
1	$P(OCH_2)_3CEt$	1946.6	1633			101	1.74	31.20
2	$P(OEt)_3$	1932.0	1618	1935.1 (1952.8)	1636	109	3.31	21.60
3	$P(OBu)_3$	1931.6	1620					
4	PMe_3	1915.9	1611	1918.7	1617	118	8.65	8.55
5	PMe_2Ph	1915.9	1610	1920.2	1620	122	6.5	10.60
6	$P(OPh)_3$	1945.1	1627	1950.0	1646	128	−2.0	30.20
7	$P(Bu)_3$	1914.8	1610			136	8.43	5.25
8	PEt_2Ph	1917.2	1611			136	6.25	9.30
9	$PMePh_2$	1918.0	1613	1922.3	1617	136	4.57	12.10
10	$P(p\text{-}CF_3C_6H_4)_3$	1925.9	1617	1929.3	1633	145	−1.39 [c]	20.20
11	$P(p\text{-}ClC_6H_4)_3$	1922.3	1616	1925.8	1636	145	1.03	16.80
12	$P(p\text{-}FC_6H_4)_3$	1920.7	1615	1924.2	1631	145	1.97	15.70
13	PPh_3	1918.9	1615	1922.5	1632	145	2.73	13.25
14	$P(p\text{-}MeC_6H_4)_3$	1917.5	1615	1920.8	1631	145	3.84	11.50
15	$P(p\text{-}OMeC_6H_4)_3$	1915.3	1613	1919.3	1631	145	4.59	10.50
16	$P(p\text{-}Me_2NC_6H_4)_3$	1910.5	1598 [d]	1915.0	1660 [d]	145	8.65	5.25
17	$PBzPh_2$	1919.8 (1935.2) [e]	1612	1938.9 1922.8	1617	152		12.30
18	$P(m\text{-}MeC_6H_4)_3$	1917.3	1615	1921.1	1632	165	3.30	
19	$P(C_6H_{11})_3$	1908.6	1613	1912.7	1626	170	9.70	1.40

[a] Tolman cone angles, degrees [8a]; [b] Values are taken from ref. 5a; [c] p$K_{a'}$, taken from ref. 8c; [d] Very strong, COMe + C_6H_4; [e] Shoulder.

four indenyl protons H(4–7) give rise to four separate signals of the type AA′BB′, or two doublets for the protons 4,7 and two triplets for the protons 5,6, as in the case of **4a** (L = PMe_3); the three protons H(1–3) give rise to three separate multiplets or singlets. The two methyl groups of $CHMe_2$ produce two doublets at about $\delta = 1$. It is noteworthy that in the case of the triarylphosphine complexes **10–16a**, one doublet is shifted to unusually high field, for instance to δ 0.13 for L = PPh_3 in $CDCl_3$. In the ^1H NMR spectra of $[(C_9H_7)Fe(CO)(COCHMe_2)(PPh_3)]$ in toluene-d_8 between 40°C and 75°C, the two doublets of the isopropyl group at 1.11 δ and 0.42 δ do not show any broadening effect and move together by only 1 Hz at the higher temperature. Diastereotopic shielding by an asymmetric iron atom in cyclopentadienyl complexes $[(C_5H_5)Fe(CO)(COR)(L)]$ has been described in the literature [10].

2.2. The molecular structure of $[(C_9H_7)Fe(CO)(COCHMe_2)(PPh_3)]$

Crystals suitable for X-ray analysis (Table 2) were obtained by slow vapour diffusion of pentane into a concentrated toluene solution at −20°C. The structure of $[(C_9H_7)Fe(CO)(COCHMe_2)(PPh_3)]$ is shown in Fig. 1. A view of a part of the complex down the normal to the plane of the five-membered ring is shown in Fig. 2, where the centroid of the ring is indicated by a dot. Fractional atomic coordinates are reported in Table 3. Selected interatomic bond distances, angles, and torsion angles are presented in Table 4. The molecule exhibits the usual localized allylene structure of η^5-indenyl in the pseudo-octahedral "three-legged piano stool" geometry. Two of the three ligand–iron–ligand bond angles are larger than 90°, the largest deviation from 90° being 4.8°. The iron–CO bond distance (1.738(2) Å) is significantly shorter than the iron–$COCHMe_2$ distance (1.956(3) Å). The Fe–P bond length is 2.214(1) Å, similar to the value 2.202(2) Å of the cyclopentadienyl complex $[(Cp)Fe(CO)(COMe)(PPh_3)]$ [5b].

The distance of the iron atom from the ring centroid is 1.797 Å. The projection of the iron atom onto the plane of the five-membered ring of the indenyl ligand is 0.19(2) Å away from the ring centroid. The five-carbon ring is planar to within 0.04 Å, while the entire ligand is planar to within 0.07 Å. The dihedral angle between the allyl and arene planes is 6.3(2)°, which is well within the range of an η^5-structure ($\Omega \leq 20°$) [11]. However the slip value, Δ = mean d[M–C(3a,7a)] − mean d[M–C(1,3)], is 0.122 Å, indicating increased distortion in the ring with respect to a nearly perfect η^5-coordination in $[(C_9H_7)_2Fe]$ ($\Delta = 0.0495$ Å) [6]. In complex **13a**, the ligand *trans* to the ene portion of the

TABLE 2. Crystal data and X-ray experimental conditions.

Formula	$C_{32}H_{29}O_2FeP$
Molecular weight	532.4
Crystal system	Triclinic
Space group	$P\bar{1}$
Cell parameters	
a(Å)	11.580(2)
b(Å)	11.372(3)
c(Å)	10.183(2)
α(°)	92.81(3)
β(°)	91.82(3)
γ(°)	101.35(4)
Volume (Å³)	1312.0
F(000)	556
Dc (g cm^{-3})	1.35
μ (cm^{-1})	6.59
Z	2
Crystal dimensions (mm)	0.08×0.11×0.16
Radiation	Mo-Kα
λ (Å)	0.71069
θ Range	3–25
Collected indices	$\pm h$, $\pm k$, $+l$
Reflections:	
total independent	4645
observed	3141
limit	$I \geq 2\sigma(I)$
No. of refined parameters: block 1	110
block 2	332
$\Delta\rho$(e Å^{-3})	0.23
Final R	0.029
Final R_w [$w = k/\sigma^2F + gF^2$)]	0.031
k	0.3077
g	0.00186

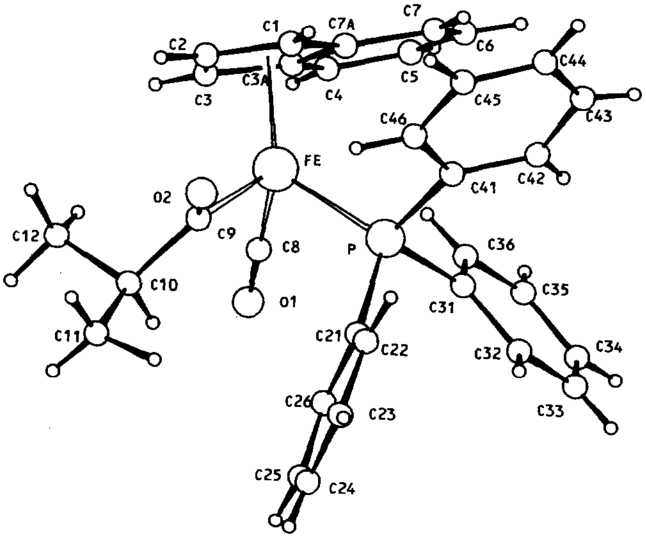

Fig. 1. Molecular structure of $[(C_9H_7)Fe(CO)(COCHMe_2)(PPh_3)]$ (**13a**).

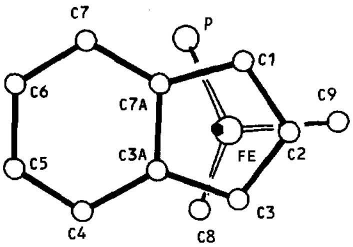

Fig. 2. A view of part of [$(C_9H_7)Fe(CO)(COCHMe_2)(PPh_3)$] along the normal to the plane of the five-membered ring. The centroid of the ring is indicated by a dot.

five-carbon ring is the acyl $COCHMe_2$. It has been observed [11] that in most structures of η^5-indenyl complexes, this position is occupied by the ligand having the largest *trans* influence [12], most likely in order to decrease ene-to-metal interaction, and to favour greater aromatization of the benzene ring. This is not the case for complex **13a**, nor for [$(C_9H_7)Ir(PMe_3)(Ph)(Me)$] [13], where the phenyl ring is *trans* to the ene bond.

With regard to the high-field chemical shift of a methyl group of $CHMe_2$ observed in ^1H and ^{13}C spectra, the structure of **13a** shows that one methyl is pointing toward the face of a phenyl ring of triphenylphosphine, the distance between C(11) and the ring centroid being 3.863 Å, and the analogous distance for C(12) being 5.567 Å. One methyl is therefore within the shielding cone of the phenyl ring. Evidently, the most stable conformation in solution closely resembles the solid-state structure.

2.3. *Analysis of ligand effects.*

The most frequently employed measure of the steric properties of phosphorus and related ligands is the cone angle, θ, as defined by Tolman [8a]. The frequency of the IR-active totally symmetric ν(CO) in $LNi(CO)_3$ complexes has been widely employed as a measure of the net relative electron density at Ni, and thus as a measure of the donor ability of L. An electronic parameter χ is associated with each ligand. Regarding the separation of electronic effects of the phosphorus ligands into the σ donor and π acceptor components, it has been shown that the χ values are a measure of σ-donicity in the cyclopentadienyliron(II) complexes [(Cp)Fe(CO)(COMe)(L)]. For those ligands that are pure σ-donors, the parameters χ correlate well with the terminal carbonyl-stretching frequencies, which are directly dependent on the electron density at the metal [5a].

A plot of carbonyl-stretching frequencies for the indenyl [$(C_9H_7)Fe(CO)(COR)(L)$] (R = $CHMe_2$ or Me) and the cyclopentadienyl complexes [$(C_5H_5)Fe(CO)(COMe)(L)$] [5a] of the isosteric ligands (L = $P(p\text{-}X\text{-}C_6H_4)_3$; X = CF_3, Cl, F, H, Me, OMe or NMe_2) *vs.* χ is shown in Fig. 3. ν(CO) correlates well with χ in all cases, and the plots have similar slopes. In the indenyl complexes, the isopropyl group produces ν(CO) at lower frequencies. This is because of its electron donor ability which increases π-back bonding from iron to carbonyl. In the methyl complexes, the ν(CO) values are virtually the same in the two series of η^5-ligands, except in the presence of the strongly electron-donating NMe_2 group, where the indenyl is an acceptor compared with Cp.

The effect of the indenyl moiety on the CO is larger in alkyl than in acyl complexes. In fact, the ν(CO) values of [$(\eta^5\text{-}L')Fe(CO)_2CHMe_2$] in hexane are 2003.7, 1950.2 cm^{-1} for L' = indenyl, and 2006.4, 1952.1 cm^{-1} for L' = cyclopentadienyl. The values for [$(\eta^5\text{-}L')Fe(CO)_2Me$] are 2011.7, 1957.9 cm^{-1} for L' =

TABLE 3. Fractional atomic coordinates ($\times 10^4$) and U_{eq} ($\times 10^4$ Å^2)

	x	y	z	U_{eq}
Fe	3495(1)	2430(1)	978(1)	310(1)
P	2787(1)	2315(1)	2972(1)	304(2)
O(1)	4726(2)	4894(2)	1516(2)	594(8)
O(2)	4626(2)	644(2)	1808(2)	490(8)
C(1)	2422(3)	922(2)	−64(3)	422(10)
C(2)	3467(3)	1273(3)	−710(3)	427(11)
C(3)	3559(3)	2452(3)	−1085(3)	424(9)
C(3a)	2476(2)	2817(2)	−795(3)	414(10)
C(4)	2053(3)	3871(3)	−1050(3)	536(12)
C(5)	962(4)	3949(4)	−725(4)	654(15)
C(6)	243(3)	3024(4)	−115(4)	681(16)
C(7)	618(3)	1992(4)	204(3)	567(13)
C(7a)	1767(2)	1862(2)	−152(3)	416(9)
C(8)	4246(2)	3900(2)	1317(3)	372(10)
C(9)	4798(2)	1702(3)	1585(3)	379(10)
C(10)	6073(3)	2427(3)	1696(4)	530(12)
C(11)	6867(4)	1858(4)	2582(5)	721(18)
C(12)	6529(4)	2558(5)	314(5)	816(21)
C(21)	3852(2)	2256(2)	4321(2)	327(8)
C(22)	3863(3)	1259(3)	5054(3)	407(10)
C(23)	4728(3)	1281(3)	6025(3)	516(12)
C(24)	5577(3)	2298(3)	6285(3)	528(13)
C(25)	5572(3)	3300(3)	5591(3)	491(12)
C(26)	4725(3)	3269(3)	4609(3)	419(10)
C(31)	2193(2)	3617(2)	3568(3)	341(9)
C(32)	2051(3)	3858(3)	4905(3)	463(12)
C(33)	1626(3)	4858(3)	5325(4)	558(14)
C(34)	1345(3)	5633(3)	4442(4)	562(12)
C(35)	1469(3)	5405(3)	3133(4)	501(13)
C(36)	1898(2)	4406(2)	2686(3)	391(10)
C(41)	1577(3)	1039(2)	3157(3)	405(10)
C(42)	442(3)	1185(3)	3403(3)	521(13)
C(43)	−472(4)	188(5)	3397(4)	741(17)
C(44)	−259(5)	−937(5)	3177(4)	836(20)
C(45)	843(6)	−1098(4)	2958(4)	762(18)
C(46)	1775(3)	−121(3)	2914(3)	535(13)

indenyl, and 2014.6, 1961.2 cm^{-1} for L′ = cyclopentadienyl. These data indicate that the indenyl in alkyl complexes is electron-donating compared with the cyclopentadienyl.

A plot of the carbonyl-stretching frequencies for the indenyl phosphine complexes [$(C_9H_7)Fe(CO)(COR)(L)$] (R = $CHMe_2$ or Me) *vs.* the χ values (Fig. 4) is linear with little scatter and a slope (0.9), similar to the plots for the complexes with the isosteric ligands (1). The plot does not include the complexes with the phosphites, $P(OR)_3$, which are strong π-acceptors, and fail to correlate well with ligands that are essentially σ-donors [5a]. The complex with the largest ligand, PCy_3, (**19**, $\theta = 170°$) fits the plot well. This indicates that the phosphorus ligands in the indenyl complexes exert effects over the molecule that are essentially electronic in nature, in spite of the crowding caused by the indenyl and the $COCHMe_2$ groups.

3. Conclusions

The effect of phosphorus ligands on the frequency ν(CO) values in [$(\eta^5\text{-}L')Fe(CO)(COMe)(L)$] is virtually independent of the group L′ (indenyl or cyclopentadienyl). In contrast, substitution of Me for $CHMe_2$ in the acyl moiety of the indenyl complexes enhances π-back-bonding from iron to carbonyl.

TABLE 4. Selected bond distances (Å), bond angles (°) and torsion angles (°)

Fe-P	2.214(1)	C(1)-C(2)	1.394(5)
Fe-C(8)	1.738(2)	C(1)-C(7a)	1.432(4)
Fe-C(9)	1.956(3)	C(2)-C(3)	1.397(5)
Fe-C(2)	2.108(3)	C(3)-C(3a)	1.431(5)
Fe-C(3)	2.106(3)	C(3a)-C(4)	1.413(5)
Fe-C(3a)	2.234(3)	C(3a)-C(7a)	1.427(4)
Fe-C(7a)	2.240(3)	C(4)-C(5)	1.335(6)
Fe-C(1)	2.124(3)	C(5)-C(6)	1.392(6)
P-C(21)	1.829(3)	C(6)-C(7)	1.379(7)
P-C(31)	1.837(3)	C(7)-C(7a)	1.423(4)
P-C(41)	1.830(3)	C(9)-C(10)	1.541(4)
O(1)-C(8)	1.162(3)	C(10)-C(11)	1.522(6)
O(2)-C(9)	1.214(4)	C(10)-C(12)	1.523(7)
P-Fe-C(9)	89.5(1)	C(6)-C(7)-C(7a)	118.2(3)
P-Fe-C(8)	92.2(1)	C(3a)-C(7a)-C(7)	118.2(2)
C(8)-Fe-C(9)	94.8(1)	C(7)-C(7a)-C(1)	134.3(2)
Fe-P-C(31)	115.3(1)	C(3a)-C(7a)-C(1)	107.4(2)
Fe-P-C(21)	116.1(1)	Fe-C(8)-O(1)	177.9(2)
Fe-P-C(41)	114.7(1)	Fe-C(9)-O(2)	120.3(2)
C(31)-P-C(41)	103.7(1)	O(2)-C(9)-C(10)	118.4(3)
C(21)-P-C(41)	105.3(1)	Fe-C(9)-C(10)	121.1(2)
C(21)-P-C(31)	99.8(1)	C(9)-C(10)-C(12)	108.3(3)
C(1)-C(2)-C(3)	109.7(3)	C(9)-C(10)-C(11)	112.2(3)
C(2)-C(3)-C(3a)	107.6(3)	C(11)-C(10)-C(12)	111.9(3)
C(3)-C(3a)-C(7a)	107.3(2)	P-C(21)-C(26)	117.6(2)
C(3)-C(3a)-C(4)	132.0(2)	P-C(21)-C(22)	124.6(2)
C(4)-C(3a)-C(7a)	120.7(2)	P-C(31)-C(36)	119.9(2)
C(3a)-C(4)-C(5)	119.3(3)	P-C(31)-C(32)	121.9(2)
C(4)-C(5)-C(6)	121.3(4)	P-C(41)-C(46)	118.8(2)
C(5)-C(6)-C(7)	122.3(3)	P-C(41)-C(42)	122.3(2)
C(8)-Fe-C(9)-C(10)	−20.1(3)	Fe-P-C(41)-C(46)	59.8(3)
P-Fe-C(9)-C(10)	−112.3(3)	Fe-P-C(31)-C(32)	−160.1(2)
C(8)-Fe-C(9)-O(2)	164.4(3)	Fe-P-C(31)-C(36)	18.4(3)
P-Fe-C(9)-O(2)	72.2(3)	Fe-P-C(21)-C(22)	−111.7(3)
C(8)-Fe-P-C(41)	165.7(2)	Fe-P-C(21)-C(26)	66.7(3)
C(8)-Fe-P-C(31)	45.3(2)	O(2)-C(9)-C(10)-C(11)	−23.0(5)
C(8)-Fe-P-C(21)	−70.9(2)	Fe-C(9)-C(10)-C(11)	161.3(3)
C(9)-Fe-P-C(41)	−99.5(2)	O(2)-C(9)-C(10)-C(12)	101.0(4)
C(9)-Fe-P-C(31)	140.1(2)	Fe-C(9)-C(10)-C(12)	−74.7(4)
C(9)-Fe-P-C(21)	23.8(2)		

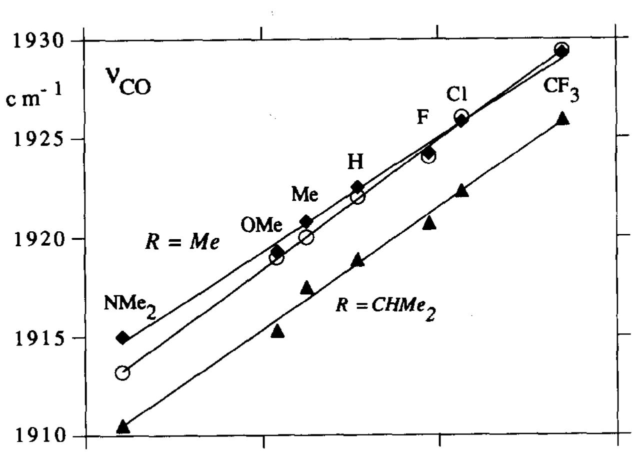

Fig. 3. Plot of the terminal carbonyl-stretching frequencies, ν(CO) (cm^{-1}), of [$(C_9H_7)Fe(CO)(COR)\{P(p\text{-}X\text{-}C_6H_4)_3\}$] (R = CHMe$_2$ (▲), R = Me (◆)) and of [$(C_5H_5)Fe(CO)(COMe)\{P(p\text{-}X\text{-}C_6H_4)_3\}$] (○) *vs.* the χ values for [$Ni(CO)_3\{P(p\text{-}X\text{-}C_6H_4)_3\}$] (X = CF$_3$, Cl, F, H, Me, OMe or NMe$_2$), taken from ref. 5b.

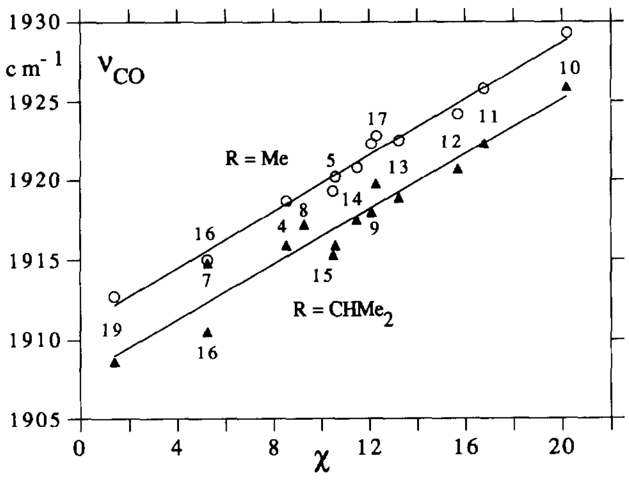

Fig. 4. Plot of ν(CO) (cm^{-1}), of [$(C_9H_7)Fe(CO)(COR)(L)$] (R = CHMe$_2$ (▲), R = Me (○); L = **4–19**) *vs.* the χ values for [$Ni(CO)_3(L)$].

The effect of changing indenyl for cyclopentadienyl, negligible in the acyl species, shows itself in the alkyl complexes [$(\eta^5\text{-}L')Fe(CO)_2R$] (L′ = C_9H_7 or C_5H_5; R = CHMe$_2$ or Me), in which C_9H_7 is an electron donor.

4. Experimental details

^{1}H NMR spectra were recorded on a Bruker WP-80, and ^{13}C spectra on a Varian XL-300 spectrometer. Chemical shifts (ppm) are relative to tetramethylsilane. IR spectra were measured with a Nicolet 510 FT-IR spectrophotometer interfaced to a 620 work station, in the solvent subtraction mode, using 0.1 mm CaF$_2$ cells. Elemental analyses were performed by the Servizio Microanalisi del CNR, Area della Ricerca di Roma, Montelibretti.

Unless otherwise indicated, all reactions were carried out under argon using standard Schlenk-line techniques. Toluene was distilled under di-nitrogen from sodium benzophenone. Hexane was distilled from sodium. Alumina (3% water) was used for chromatography. Chemicals and solvents were reagent grade. [$\{(C_5H_5)Fe(CO)_2\}_2$] was commercially available (Aldrich) and [$\{(C_9H_7)Fe(CO)_2\}_2$] was prepared as described in the literature [14]. [$(C_5H_5)Fe(CO)_2R$] (R = CHMe$_2$ or Me) were prepared as described [15].

4.1. [$(C_9H_7)Fe(CO)_2CHMe_2$]

[$\{(C_9H_7)Fe(CO)_2\}_2$] (9.12 g, 20 mmol) was reduced with sodium amalgam (1.0 g sodium in 8 ml mercury) in THF (150 ml), and the resulting anion allowed to react for 4 h with isopropyl bromide (5.4 g, 44 mmol). After evaporation of the solvent, the crude product was extracted with hexane, and the extracts chromatographed on alumina to give 2.1 g of product (20%) as a dark-orange oil that became solid at low temperature. It was stored at 0°C. IR ν(CO) (CH_2Cl_2): 1996, 1939.3 cm^{-1}. ^{1}H NMR (C_6D_6): δ 7.3–6.7 (m, 4H, benzo); 4.80 (d, 2H, J = 2.8 Hz, H(1,3)); 4.23 (tr, 1H, J = 2.9 Hz, H(2)); 2.10 (septet, 1H, J = 6.8 Hz, CHMe$_2$); 1.32 (d, 6H, J = 6.5 Hz, Me$_2$).

*4.2. [$(C_9H_7)Fe(CO)(PPh_3)(COCHMe_2)$] (**13a**)*

[$(C_9H_7)Fe(CO)_2CHMe_2$] (45 mg, 0.16 mmol) and PPh$_3$ (87 mg, 0.33 mmol) were stirred in toluene (30 ml) at 40°C (18 h). The solvent was removed under vacuum, and the residue chromatographed eluting first with hexane and then with hexane–dichloromethane to give an orange-red solid (50 mg, 60%). IR (CH_2Cl_2): 1911.1 (CO); 1606.1 (C=O) cm^{-1}.

The acyl complexes were prepared as described for **13a**, in toluene, with the phosphine in about 10% excess, and following the reaction, by infrared spectroscopy until completion. The complexes were purified by column chromatography by elution with CH_2Cl_2 or THF, and obtained with yields around 60%. Analytically pure samples were obtained by slow vapour-diffusion of pentane into a toluene solution of the complex at −20°C. NMR and analytical data for the acetyl complexes **2–19b** have been reported elsewhere [16]. NMR ($CDCl_3$) spectra and analytical data of complexes **1–19a** are as follows:

[$(C_9H_7)Fe(CO)(COCHMe_2)\{P(OCH_2)_3CEt\}$] (**1a**). Yellow brown solid. ^{1}H NMR: δ 7.3–7.0 (AA′BB′, $H_4 - H_7$); 5.40, 5.30 (bs, Ind $H_{1,3}$); 4.87 (t, J(HH) = 2.8 Hz, Ind H_2); 4.11 (d, J(PH) = 4.2 Hz, $P(OCH_2)_3CEt$);

2.94 (septet, 1H, *J*(HH) = 6.8 Hz, C*H*Me$_2$); 1.15 (q, *J*(HH) = 7.7 Hz, P(OCH$_2$)$_3$CC*H*$_2$Me); 1.01 (d, 3H, *J*(HH) = 7.0 Hz, CH*Me*); 080 (d, 3H, *J*(HH) = 6.8 Hz, CH*Me*); 0.78 ppm (t, *J*(HH) = 7.7 Hz, P(OCH$_2$)$_3$C-CH$_2$*Me*). ^{13}C NMR: δ 271.94 (d, *J*(PC) = 36.7 Hz, C=O); 217.77 (d, *J*(PC) = 40.1 Hz, CO); 125.62, 125.00, 124.79, 124.09 (Ind C$_4$–C$_7$); 106.01, 103.76 (Ind C$_{3a}$ + C$_{7a}$); 100.35 (s, Ind C$_2$); 74.35 (d, *J*(PC) = 4.6 Hz, P(O*C*H$_2$)$_3$CEt); 73.57, 70.52 (Ind C$_{1,3}$); 69.84 (d, *J*(PC) = 4.6 Hz, P(OCH$_2$)$_3$*C*Et); 61.41 (d, *J*(PC) = 5.8 Hz, *C*HMe$_2$); 23.35 (P(OCH$_2$)$_3$C*C*H$_2$Me); 18.69–18.64 (CH*Me*$_2$); 7.05 (P(OCH$_2$)$_3$CCH$_2$*Me*). Anal. Found: C, 55.39; H, 6.02. $C_{20}H_{25}O_5PFe$ calc.: C, 55.57; H, 5.82%. Melting point: 115–118°C.

[(C$_9$H$_7$)Fe(CO)(COCHMe$_2$){P(OEt)$_3$}] (**2a**). Oil. ^{1}H NMR: δ 7.38 – 6.97 (AA'BB', Ind H$_7$–H$_4$); 5.34, 5.28 (bs, Ind H$_{1,3}$); 4.95 (t, *J*(HH) = 2.9 Hz, Ind H$_2$); 3.78 (m, P(OC*H*$_2$Me)$_3$); 3.45 (m, P(OC*H*$_2$Me)$_3$); 3.02 (septet, 1H, *J*(HH) = 6.8 Hz, C*H*Me$_2$); 1.19 (t, *J*(HH) = 7.0 Hz, P(OCH$_2$*Me*)$_3$); 1.05 (d, 3H, *J*(HH) = 7.05 Hz, CH*Me*); 0.80 (d, *J*(HH) = 6.5 Hz, 3H, CH*Me*).

[(C$_9$H$_7$))Fe(CO)(COCHMe$_2$){P(OBu)$_3$}] (**3a**). Oil. ^{1}H NMR: δ 7.4–6.9 (AA'BB', Ind H$_7$–H$_4$); 5.30, 5.29 (s, 2H, Ind H$_{1,3}$); 4.94 (bs, Ind H$_2$); 3.69 (m, P[OC*H*$_2$(CH$_2$)$_2$Me]$_3$); 3.38 (m, P[OC*H*$_2$(CH$_2$)$_2$Me]$_3$); 3.01 (septet, 1H, *J*(HH) = 6.7 Hz, C*H*Me$_2$); 1.51 (m, P(OCH$_2$C*H*$_2$CH$_2$Me)$_3$); 1.35 (m, P[O(CH$_2$)$_2$-C*H*$_2$Me]$_3$); 1.05 (d, 3H, *J*(HH) = 7.1 Hz, CH*Me*); 0.91 (t, *J*(HH) = 7.3 Hz, P[O(CH$_2$)$_3$*Me*]$_3$; 0.80 (d, 3H, *J*(HH) = 7.1 Hz, CH*Me*).

[(C$_9$H$_7$)Fe(CO)(COCHMe$_2$)(PMe$_3$)] (**4a**). Oil. ^{1}H NMR: δ 7.46 (d, *J*(HH) = 8.5 Hz, Ind H$_{4\mathrm{or}7}$); 7.28 (d, *J*(HH) = 8.3 Hz, Ind H$_{4\mathrm{or}7}$); 7.05 (t, 1H, *J*(HH) = 7.5 Hz, Ind H$_{5\mathrm{or}6}$); 6.94 (t, 1H, *J*(HH) = 7.5 Hz, Ind H$_{5\mathrm{or}6}$); 5.17 (bs, Ind H$_{1,3}$); 4.97 (bs, Ind H$_{1,3}$); 4.86 (t, *J*(HH) = 2.5 Hz, Ind H$_2$); 3.16 (septet, 1H, *J*(HH) = 6.8 Hz, C*H*Me$_2$); 1.04 (d, 3H, *J*(HH) = 6.0 Hz, CH*Me*); 1.02 (d, *J*(PH) = 9.5 Hz, PMe$_3$); 0.81 (d, 3H, *J*(HH) = 6.6 Hz, CH*Me*).

[(C$_9$H$_7$)Fe(CO)(COCHMe$_2$)(PMe$_2$Ph)] (**5a**). Oil. ^{1}H NMR: δ 7.4–6.6 (m, Ind and Ph); 5.15, 4.89 (bs, Ind H$_{1,3}$); 4.84 (bs, Ind H$_2$); 3.14 (septet, 1H, *J*(HH) = 6.8 Hz, C*H*Me$_2$); 1.56 (d, 3H, *J*(PH) = 9.5 Hz, PMe); 1.13 (d, 3H, *J*(PH) = 9.0 Hz, PMe); 1.06 (d, 3H, *J*(HH) = 6.9 Hz, CH*Me*); 0.74 (d, 3H, *J*(HH) = 6.6 Hz, CH*Me*).

[(C$_9$H$_7$)Fe(CO)(COCHMe$_2$){P(OPh)$_3$}] (**6a**). Gummy Solid. ^{1}H NMR: δ 7.31–6.72 (m, Ind + phosphite); 5.10 (s, Ind H$_{1,3}$); 4.66 (d, *J* = 2.7 Hz, Ind H$_2$); 2.98 (septet, 1H, *J*(HH) = 6.8 Hz, C*H*Me$_2$); 0.99 (d, 3H, *J*(HH) = 7.0 Hz, CH*Me*); 0.75 (d, 3H, *J*(HH) = 6.6 Hz, CH*Me*).

[(C$_9$H$_7$)Fe(CO)(COCHMe$_2$)(PBu$_3$)] (**7a**). Oil. ^{1}H NMR: δ 7.5–7.0 (AA'BB', Ind H$_{4-7}$); 5.22, 5.07 (m, Ind H$_{1,3}$); 4.92 (m, Ind H$_2$); 3.24 (septet, 1H, *J*(HH) = 6.8 Hz, C*H*Me$_2$); 1.3–1.2 (m, P(C*H*$_2$)$_3$Me)$_3$); 1.06 (d, 3H, *J*(HH) = 6.9 Hz, CH*Me*); 0.88 (t, *J*(HH) = 6.7 Hz, P[(CH$_2$)$_3$*Me*]$_3$); 0.81 (d, 3H, *J*(HH) 6.6 Hz, CH*Me*).

[(C$_9$H$_7$)Fe(CO)(COCHMe$_2$)(PEt$_2$Ph)] (**8a**). Oil. ^{1}H NMR: δ 7.6–6.8 (m, Ind + PPh); 5.02, 4.73 (s, Ind H$_{1,3}$); 4.92 (t, *J* = 2.8 Hz, Ind H$_2$); 3.23 (septet, 1H, *J*(HH) = 6.8 Hz, C*H*Me$_2$); 1.80–1.58 (m, PC*H*$_2$Me); 1.44–1.24 (m, PC*H*$_2$Me); 1.06 (d, 3H, *J*(HH) = 6.9 Hz, CH*Me*); 0.79 (d, 3H, *J*(HH) = 6.9 Hz, CH*Me*); 0.84–0.64 (m, P(CH$_2$*Me*)$_2$).

[(C$_9$H$_7$)Fe(CO)(COCHMe$_2$)(PMePh$_2$)] (**9a**). ^{1}H NMR: δ 7.5–6.6 (m, Ind + PPh$_2$); 5.16, 4.95, 4.89 (s, 3H, H$_{1,2,3}$); 2.70 (septet, 1H, *J*(HH) = 6.0 Hz, C*H*Me$_2$); 1.95 (d, 3H, *J*(PH) = 8.2 Hz, PMe); 1.00 (d, 3H, *J*(HH) = 5.8 Hz, CH*Me*); 0.29 ppm (d, 3H, *J*(HH) = 5.5 Hz, CH*Me*). Anal. Found: C, 68.7; H, 5.8. $C_{27}H_{27}FeO_2P$ calc.: C, 68.9; H, 5.8%.

[(C$_9$H$_7$)Fe(CO)(COCHMe$_2$)}P(*p*-CF$_3$-C$_6$H$_4$)$_3$}] (**10a**). ^{1}H NMR: δ 7.7–6.1 (m, Ind + phosphine); 5.21, 5.14, 4.47 (s, Ind H$_{1,2,3}$); 2.93 (septet, 1H, *J*(HH) = 6.4 Hz, C*H*Me$_2$); 1.02 (d, 3H, *J*(HH) = 6.4 Hz, CH*Me*); 0.20 (d, 3H, *J*(HH) = 6.1 Hz, CH*Me*). Anal. Found: C, 57.26; H, 3.52. $C_{35}H_{26}O_2F_3PFe$ calc.: C, 57.08; H, 3.55%. Melting point: 155–156.5°C.

[(C$_9$H$_7$)Fe(CO)(COCHMe$_2$){P(*p*-Cl-C$_6$H$_4$)$_3$}] (**11a**). ^{1}H NMR (CDCl$_3$) δ: 7.60–6.16 (m, Ind + phosphine); 5.14, 5.09, 4.48 (s, 3H, Ind H$_{1,2,3}$); 2.91 (septet, 1H, *J*(HH) = 6.8 Hz, C*H*Me$_2$); 1.02 (d, 3H, *J*(HH) = 6.8 Hz, CH*Me*); 0.24 (d, *J*(HH) = 6.4 Hz, CH*Me*). Anal. Found: C, 60.74; H, 4.26. $C_{32}H_{26}O_2FeCl_3P$ calc.: C, 60.45; H, 4.12%. Melting point: 154–155.5°C.

[(C$_9$H$_7$)Fe(CO)(COCHMe$_2$){P(*p*-F-C$_6$H$_4$)$_3$}] (**12a**). ^{1}H NMR δ: 7.6–6.1 (m, Ind + phosphine); 5.14, 5.09, 4.50 (s, 3H Ind H$_{1,2,3}$); 2.91 (septet, 1H, *J*(HH) = 6.9 Hz, C*H*Me$_2$); 1.03 (d, 3H, *J*(HH) = 6.6 Hz, CH*Me*), 0.22 (d, 3H, *J*(HH) = 6.1 Hz, CH*Me*).

[(C$_9$H$_7$)Fe(CO)(COCHMe$_2$)(PPh$_3$)] (**13a**). ^{1}H NMR: δ 7.6–6.1 (m, Ind + phosphine); 5.12, 5.08 (s, 2H, Ind H$_{1,3}$); 4.56 (s, Ind H$_2$); 2.89 (septet, 1H, *J*(HH) = 6.7 Hz, C*H*Me$_2$); 1.03 (d, 3H, *J*(HH) = 6.9 Hz, CH*Me*); 0.13 (d, 3H, *J*(HH) = 6.4 Hz, CH*Me*). ^{13}C NMR: δ 279.60 (d, *J*(PC) = 20.4 Hz, C=O); 221.29 (d, *J*(PC) = 23.8 Hz, CO); 133.75 (d, *J*(PC) = 35.6 Hz, PPh$_3$ C$_{ipso}$); 129.53–127.75–127.62 (PPh$_3$); 126.30, 125.41, 124.54, 122.32 (Ind C$_{4-7}$); 110.91, 104.96 (Ind C$_{3a,7a}$); 99.67 (Ind C$_2$); 79.13–66.19 (Ind C$_{1,3}$); 61.14 (d, *J*(PC) = 5.5 Hz, *C*HMe$_2$); 19.42, 18.19 (CH*Me*$_2$).

[(C$_9$H$_7$)Fe(CO)(COCHMe$_2$){P(*p*-Me-C$_6$H$_4$)$_3$}] (**14a**). ^{1}H NMR: δ 7.55–6.13 (m, Ind + phosphine); 5.08, 5.05 (s, 2H, Ind H$_{1,3}$); 4.57 (s, Ind H$_2$); 2.87 (septet, 1H, *J*(HH) = 6.8 Hz, C*H*Me$_2$); 2.32, (s, P(*p*-*Me*-C$_6$H$_4$)$_3$); 1.03 (d, 3H, *J*(HH) = 7.1 Hz, CH*Me*); 0.15 (d, 3H, *J*(HH) = 6.5 Hz, CH*Me*).

[(C$_9$H$_7$)Fe(CO)(COCHMe$_2$){P(*p*-OMe-C$_6$H$_4$)$_3$}]

(15a). ^{1}H NMR: δ 7.6–6.1 (m, Ind + phosphine); 5.09, 5.07 (s, Ind $H_{1,3}$); 4.58 (d, $J = 0.5$ Hz, Ind H_2); 3.79 (s, O*Me*); 2.88 (septet, 1H, J(HH) = 6.7 Hz, C*H*Me$_2$); 1.03 (d, 3H, J(HH) = 7.1 Hz, CH*Me*); 0.19 (d, 3H, J(HH) = 6.4 Hz, CH*Me*).

$[(C_9H_7)Fe(CO)(COCHMe_2)\{P(p\text{-}NMe_2\text{-}C_6H_4)_3\}]$ **(16a)**. ^{1}H NMR: δ 7.5–6.5 (m, Ind + phosphine); 5.04 (s, Ind $H_1 + H_3$); 4.67 (s, Ind H_2); 2.93 (s, $N(CH_3)_2$); 2.84 (septet, 1H, J(HH) = 6.8 Hz, C*H*Me$_2$); 1.04 (d, 3H, J(HH) = 7.1 Hz, CH*Me*); 0.15 (d, 3H, J(HH) = 6.5 Hz, CH*Me*). Anal. Found: C, 67.18; H, 6.08; N, 5.75. $C_{38}H_{44}O_2N_3PFe$ calc.: C, 68.35; H, 6.75; N, 6.34%. Decomposes above 180°C.

$[(C_9H_7)Fe(CO)(COCHMe_2)(PBzPh_2)]$ **(17a)**. ^{1}H NMR: δ 7.5–6.5 (m, Ind + phosphine); 5.02, 4.98 (m, 2H, Ind $H_{1,3}$); 4.53 (m, Ind H_2); 3.62 (dd, 1H, J(PH) = 8.7 Hz, J(HH) = 14.1 Hz, PC*H*HPh); 3.20 (dd, 1H, J(PH) = 8.3 Hz, J(HH) = 13.9 Hz, PCH*H*Ph); 3.09 (septet, 1H, J(HH) = 6.8 Hz, C*H*Me$_2$); 1.06 (d, 3H, J(HH) = 6.9 Hz, CH*Me*); 0.64 (d, 3H, J(HH) = 6.6 Hz, CH*Me*). Anal. Found: C, 73.10; H, 6.07. $C_{33}H_{31}O_2PFe$ calc.: C, 72.53; H, 5.7%. Melting point: 158.5–160°C.

$[(C_9H_7)Fe(CO)(COCHMe_2)\{P(m\text{-}Me\text{-}C_6H_4)_3\}]$ **(18a)**. Oil. ^{1}H NMR: δ 7.6–6.1 (m, Ind + phosphine); 6.06, 5.08 (m, Ind $H_{1,3}$); 4.52 (bs, Ind H_2); 2.93 (septet, 1H, J(HH) = 6.7 Hz, C*H*Me$_2$); 2.29 (s, *m*-Me); 1.04 (d, 3H, J(HH) = 7.1 Hz, CH*Me*); 0.19 (d, 3H, J(HH) = 6.5 Hz, CHMe).

$[(C_9H_7)Fe(CO)(COCHMe_2)\{P(C_6H_{11})_3\}]$ **(19a)**. ^{1}H NMR: δ 7.4–6.9 (m, Ind H_7–H_4); 5.90 (d, $J = 1.1$ Hz, Ind $H_{1\,or\,3}$); 5.02 (d, $J = 0.4$ Hz, Ind $H_{1\,or\,3}$); 4.82 (d, $J = 0.9$ Hz, H_2); 3.25 (bt, J(HH) = 6.3 Hz, C*H*Me$_2$); 1.9–1.15 (m, $P(C_6H_{11})_3$); 1.08 (d, 3H, J(HH) = 6.9 Hz, CH*Me*); 0.84 (d, 3H, J(HH) = 6.1 Hz, CH*Me*). ^{13}C NMR: δ 280.95 (d, J(PC) = 19.4 Hz, C=O); 225.39 (d, J(PC) = 22.6 Hz, CO); 124.91–124.76–123.66–123.38 (Ind C_4–C_7); 110.14, 109.01 (Ind $C_{3a} + C_{7a}$); 100.28 (Ind C_2); 72.01, 64.31 (Ind $C_1 + C_3$); 60.71 (d, J(PC) = 4.5 Hz, *C*HMe$_2$); 37.5–26.6 (m, $P(C_6H_{11})_3$); 19.98, 19.46 (CH*Me*$_2$). Melting point: 139–142°C.

4.3. X-Ray analysis

The crystal data and details of the experimental conditions are given in Table 2. Cell parameters were obtained from least-square on angular (θ, χ, ϕ)*hkl* values of 27 reflections automatically well-centred on the diffractometer with a program that repeatedly improves the angular values to reach the maximum of the peak, until the values do not move more than 0.01° [17]. X-ray diffraction data were measured at room temperature on a Siemens AED single-crystal diffractometer equipped with a IBM PS2/30 personal computer. The possible decomposition or the misalignment of the specimen was controlled by measuring one reflection in every 50; none of these phenomena were observed during the data collection time. The intensities were converted to structure factors in a conventional manner, and corrected for Lorentz and polarization effects. The structure was solved with automated Patterson methods with XFPS90 [18] and, at the beginning, refined by full-matrix isotropic cycles of all heavy atoms with SHELX76 [19]. The absorbtion correction was performed with the program DIFABS [20]. After some block-matrix anisotropic cycles, all the H atoms were found in a ΔF map and refined isotropically. All the calculations were performed on an IBM PS2/80 personal computer with the CRYSRULER package [21]. The final atomic coordinates are in Table 3. Calculated and observed structure factors, anisotropic thermal parameters and hydrogen atoms coordinates are available from one of the authors (G.B.) on request.

Acknowledgments

A grant from NATO is gratefully acknowledged (Collaborative Research Grant 900289). We wish to thank Dr. L. Petrilli and Mr. F. Dianetti for the microanalysis measurements.

References

1 (a) A.J. Hart-Davis, C. White and R.J. Mawby, *Inorg. Chim. Acta, 4* (1970) 441; (b) P. Caddy, M. Green, E. O'Brien, L.E. Smart and P. Woodward, *J. Chem. Soc., Dalton Trans.*, (1980) 962; (c) M.E. Rerek and F. Basolo, *J. Am. Chem. Soc., 106* (1984) 5908; (d) G.K. Yang and R.G. Bergman, *Organometallics, 4* (1985) 129; (e) C.P. Casey, J.M. O'Connor, W.D. Jones and K.J. Haller, *Organometallics, 2* (1983) 535; (f) C.P. Casey and J.M. O'Connor, *Organometallics, 4* (1985) 384; (g) A. Habib, R.S. Tanke, E.M. Holt and R.H. Crabtree, *Organometallics, 8* (1989) 1225; (h) A.K. Kakkar, N.J. Taylor and T.B. Marder, *Organometallics, 8* (1989) 1765; (i) H. Bang, T.J. Lynch and F. Basolo, *Organometallics, 11* (1992) 40.

2 (a) A.J. Hart-Davis and R.J. Mawby, *J. Chem. Soc. A*, (1969) 2403; (b) T.C. Forschner and A.R. Cutler, *Organometallics, 4* (1985) 1247.

3 J.M. O'Connor and C.P. Casey, *Chem. Rev., 87* (1987) 307.

4 G.J. Kubas, G. Kiss and C.D. Hoff, *Organometallics, 10* (1991) 2870.

5 (a) M.M. Rahman, H.Y. Liu, K. Eriks, A. Prock and W.P. Giering, *Organometallics, 8* (1989) 1; (b) H.Y. Liu, K. Eriks, A. Prock and W.P. Giering, *Organometallics, 9* (1990) 1758.

6 S.A. Westcott, A.K. Kakkar, G. Stringer, N.J. Taylor and T.B. Marder, *J. Organomet. Chem., 394* (1990) 777.

7 (a) J.A. Collman, L.S. Hegedus, J.R. Norton and R.G. Finke, *Principles and Applications of Organotransition Metal Chemistry*, University Science Books, Mill Valley, CA, 1987; (b) A. Prock, W.P. Giering, J.E. Greene, R.E. Meirowitz, S.L. Hoffman, D.C. Woska, M. Wilson, R. Chang, J. Chen, R.H. Magnuson and K. Eriks, *Organometallics, 10* (1991) 3479.

8 (a) C.A. Tolman, *Chem. Rev., 77* (1977) 313; (b) T.L. Brown, *Inorg. Chem., 31* (1992) 1286; (c) A.J. Poe, D.H. Farrar and Y. Zheng, *J. Am. Chem. Soc., 114* (1992) 5146.

9 J.D. Cotton, G.T. Crisp and L. Latif, *Inorg. Chim. Acta, 47* (1981) 171.

10 (a) M. Green and D.J. Westlake, *J. Chem. Soc. A*, (1971) 367; (b) J.W. Faller and A.S. Anderson, *J. Am. Chem. Soc., 91* (1969) 1550; (c) K.H. Pannell, *Chem. Commun.*, (1969) 1346; (d) H. Brunner and E. Schmidt, *Angew. Chem., Int. Ed. Engl., 8* (1969) 616.

11 J.W. Faller, R.H. Crabtree and A. Habib, *Organometallics, 4* (1985) 929.

12 F.A. Cotton and G. Wilkinson, *Advanced Inorganic Chemistry*, 5th edn., Wiley, New York, 1988, p. 1299.

13 T. Foo and R.G. Bergman, *Organometallics, 11* (1992) 1801.

14 T.C. Forschner and A.R. Cutler, *Inorg. Chim. Acta, 102* (1985) 113.

15 J.P. Bibler and A. Wojcicki, *Inorg. Chem., 5* (1966) 889.

16 D. Monti and M. Bassetti, *J. Am. Chem. Soc., 115* (1993) 4658; M. Bassetti, D. Monti and L. Mannina, in preparation.

17 D. Belletti, A. Cantoni and G. Pasquinelli, *Gestione on line di diffrattometro a cristallo singolo Siemens AED con sistema IBM PS2/30*. Centro di Studio per la Strutturistica Diffrattometrica del C.N.R. Parma, Internal report, 1988.

18 F. Pavelcik, J. Sivy, C. Rizzoli and G.D. Andretti, *J. Appl. Crystallogr., 25* (1992) 328.

19 G.M. Sheldrick, *SHELX76, Program for crystal structure determination*, Univ. of Cambridge, England, 1976.

20 P. Gluzinski, *XRAY, Set of programs for X-ray structural calculations*, Polish Academy of Sciences, Warszawa, Poland, 1989.

21 C. Rizzoli, V. Sangermano, G. Calestani and G.D. Andretti, *J. Appl. Crystallogr., 20* (1987) 436.